

Ruthenium-containing P450 inhibitors for dual enzyme inhibition and DNA damage

Ana Zamora,^{b,†} Catherine A. Denning,^{a,†} David K. Heidary,^a Erin Wachter,^a Leona A. Nease,^a José Ruiz^b and Edith C. Glazer^{a*}.

^aUniversity of Kentucky, Lexington, KY 40506, United States

^bDepartamento de Química Inorgánica and Regional Campus of International Excellence “Campus Mare Nostrum”, Universidad de Murcia, and Institute for Bio-Health Research of Murcia (IMIB-Arrixaca), E-30071 Murcia, Spain

[†]Authors contributed equally to this work.

Contents:

Table S1. HPLC method 1.

Table S2. HPLC method 2.

Figure S1. ¹H NMR in CD₃CN for **3**.

Figure S2. ¹³C NMR in CD₃CN for **3**.

Figure S3. ¹H NMR in CD₃CN for **4**.

Figure S4. ¹³C NMR in CD₃CN for **4**.

Figure S5. Thermal stability for complexes **2–4**.

Figure S6. Photoejection of **2** followed by UV/Vis absorption spectroscopy in different media.

Figure S7. Photoejection of **3** followed by UV/Vis absorption spectroscopy in different media.

Figure S8. Photoejection of **4** followed by UV/Vis absorption spectroscopy in different media.

Table S3. Half-lives (*t*_{1/2}) for photoejection for **2**.

Table S4. Δ_{abs} of photoejection for **3**.

Table S5. Δ_{abs} of photoejection for **4**.

Figure S9. HPLC chromatograms of **2** in the dark and after 1 min irradiation with 470 nm light.

Figure S10. ESI-MS of **2** after being irradiated with 470 nm light.

Figure S11. HPLC chromatograms of **3** in the dark and after 1 min irradiation with 470 nm light.

Figure S12. ESI-MS of **3** after being irradiated with 470 nm light.

Figure S13. HPLC chromatograms of **4** in the dark and after 1 min irradiation with 470 nm light.

Figure S14. ESI-MS of **4** after being irradiated with 470 nm light.

Figure S15. P450_{BM3} binding titrations for each ligand.

Figure S16. P450_{BM3} binding titrations for irradiated complexes **2–4**.

Table S6. *K*_d values for all compounds determined by optical titration.

Figure S17. Difference spectra for P450_{BM3} inhibitor saturated samples.

Figure S18. P450_{BM3} activity assay for metyrapone, etomidate, **2** and **3**.

Figure S19. Singlet Oxygen Sensor Green detection of ¹O₂.

Table S7. P450_{BM3} activity assay IC₅₀ values.

Figure S20. DNA damage assay for each ligand.

Table S1. HPLC method 1.

Time (min)	0.1% formic acid in dH ₂ O	0.1% formic acid in CH ₃ CN
0	98	2
2	95	5
5	70	30
15	70	30
20	40	60
30	5	95
35	98	2
40	98	2

Table S2. HPLC method 2.

Time (min)	0.1% formic acid in dH ₂ O	0.1% formic acid in CH ₃ CN
0	98	2
2	95	5
5	95	5
10	90	10
20	90	10
25	70	30
30	40	60
35	5	95
40	98	2
45	98	2

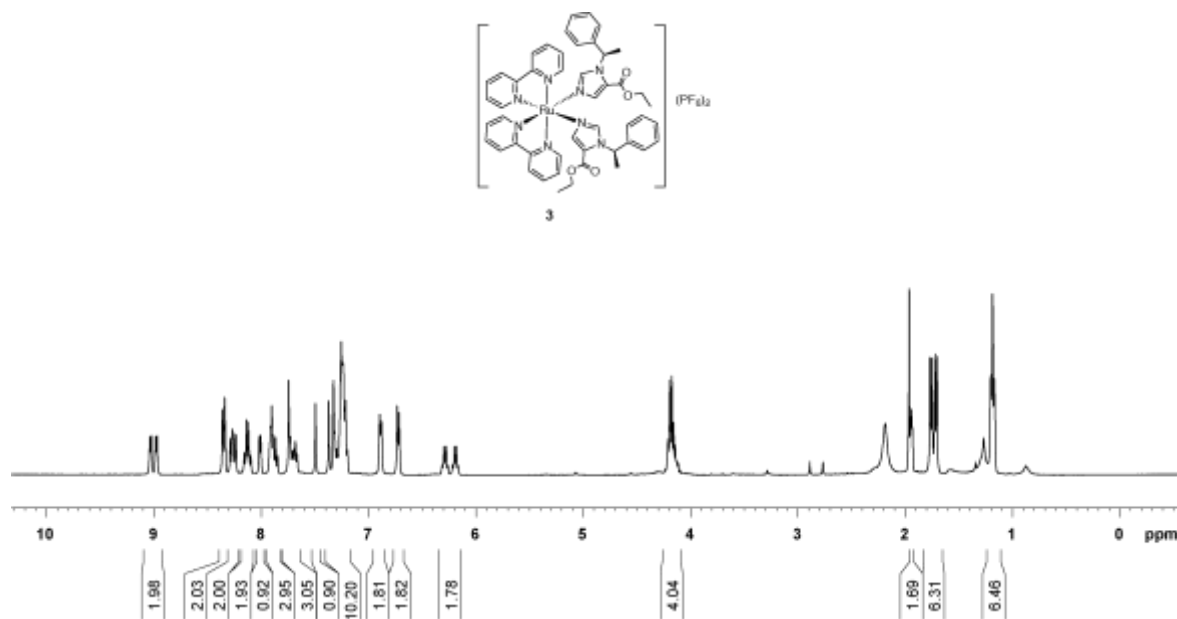


Figure S1. ¹H NMR spectrum of **3** (400 MHz, CD₃CN).

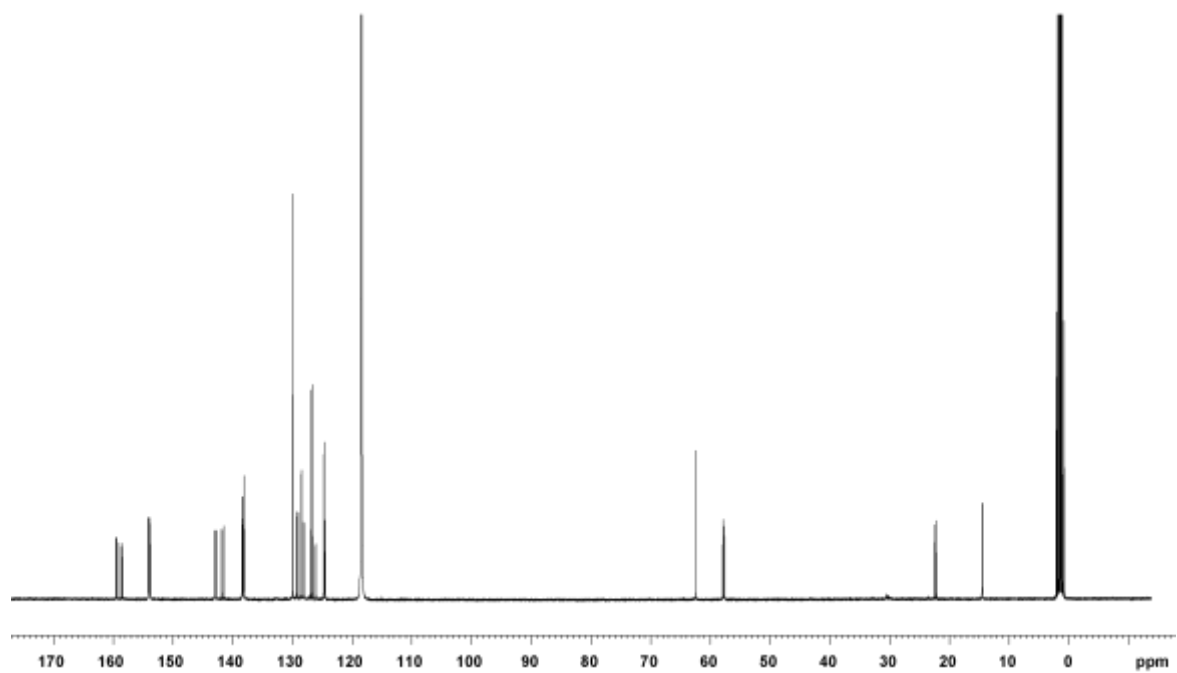


Figure S2. ¹³C NMR spectrum of **3** (100 MHz, CD₃CN).

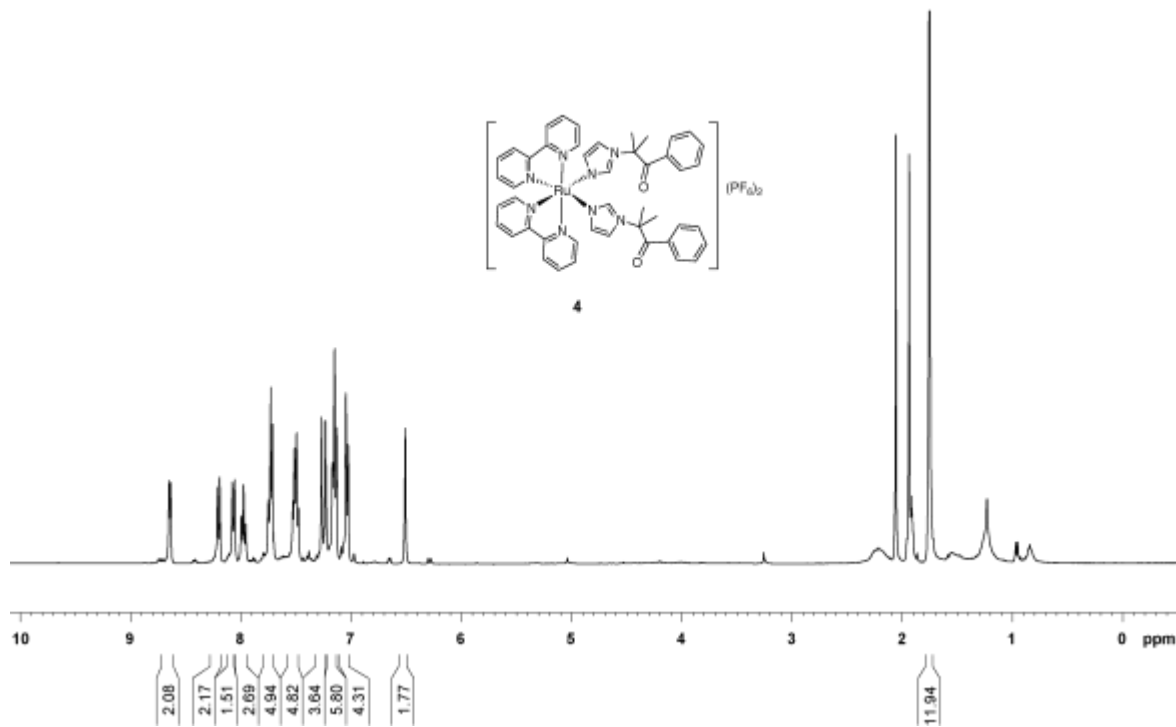


Figure S3. 1H NMR spectrum of **4** (400 MHz, CD_3CN).

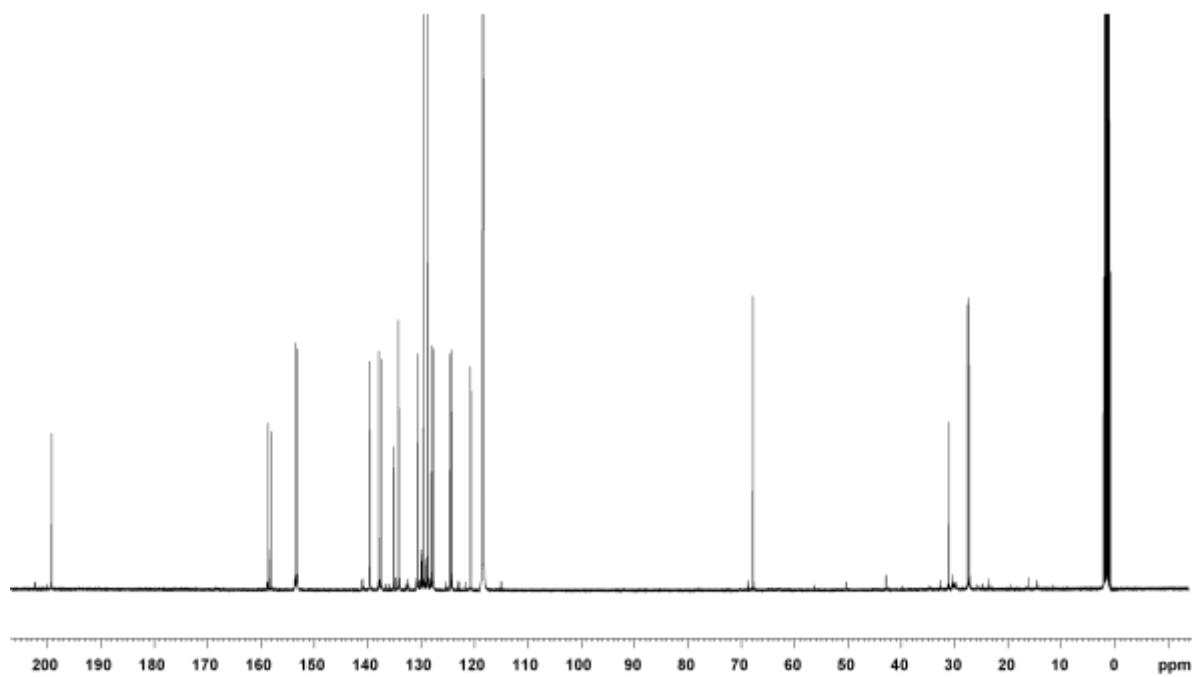


Figure S4. ^{13}C NMR spectrum of **4** (100 MHz, CD_3CN).

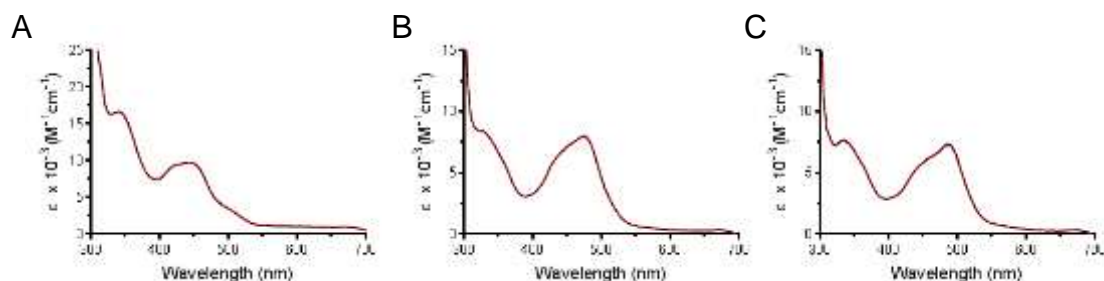


Figure S5. Thermal stability for complexes 2–4. (A) 2, (B) 3, and (C) 4 at RT (–) and 37 °C (– –) after 30 min incubation in MeCN. Studies were also performed in H₂O over 48 hours at 37 °C, and no changes were observed.

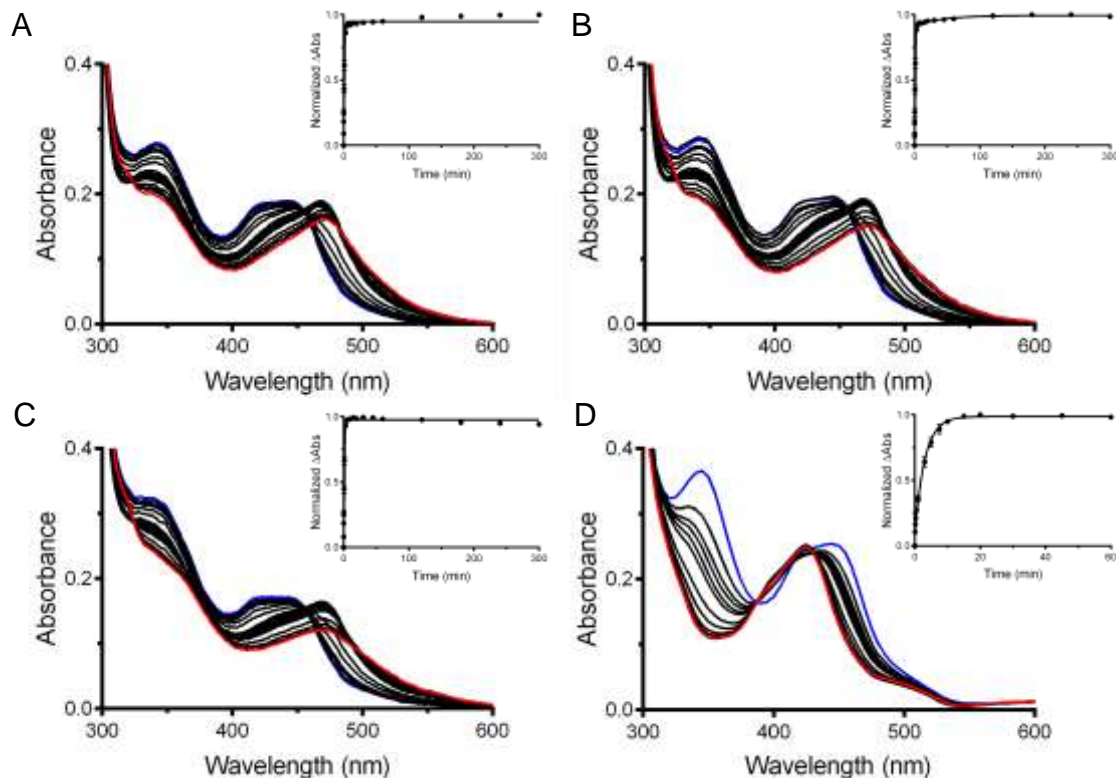


Figure S6. Photoejection of 2 (30 μ M) followed by UV/Vis absorption spectroscopy in different media; (A) water, (B) 1X PBS, (C) Opti-MEM with 1% FBS, (D) CH₃CN. The blue line is the initial and the red line is the final spectra. Inset: The kinetics curves were produced by monitoring the change in absorbance at 470–440 nm (aqueous conditions) or 425–445 nm (acetonitrile) and fit with a two phase decay non-linear equation using GraphPad Prism software.

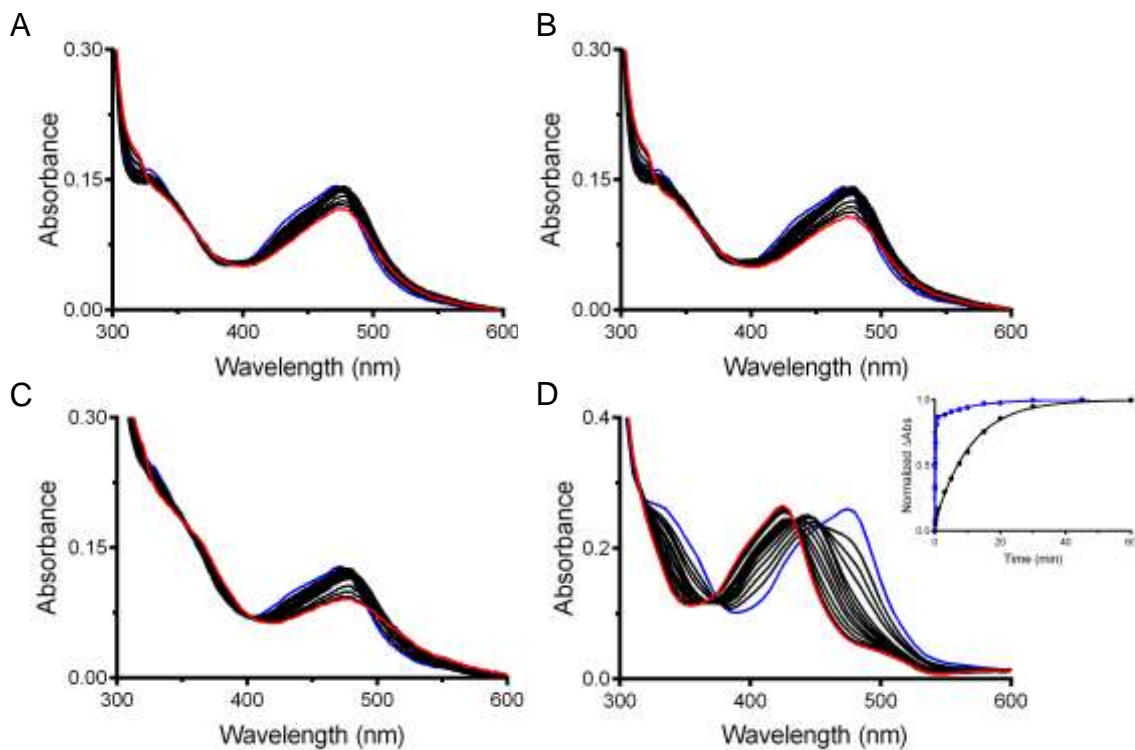


Figure S7. Photoejection of **3** (30 μ M) followed by UV/Vis absorption spectroscopy in different media; (A) water, (B) 1X PBS, (C) Opti-MEM with 1% FBS, (D) CH₃CN. The blue line is the initial and the red line is the final spectra. Inset: The kinetics curve was produced by monitoring the change in absorbance at 475-440 nm (blue) and 425-440 nm (black) and fit with a one phase decay non-linear equation using GraphPad Prism software.

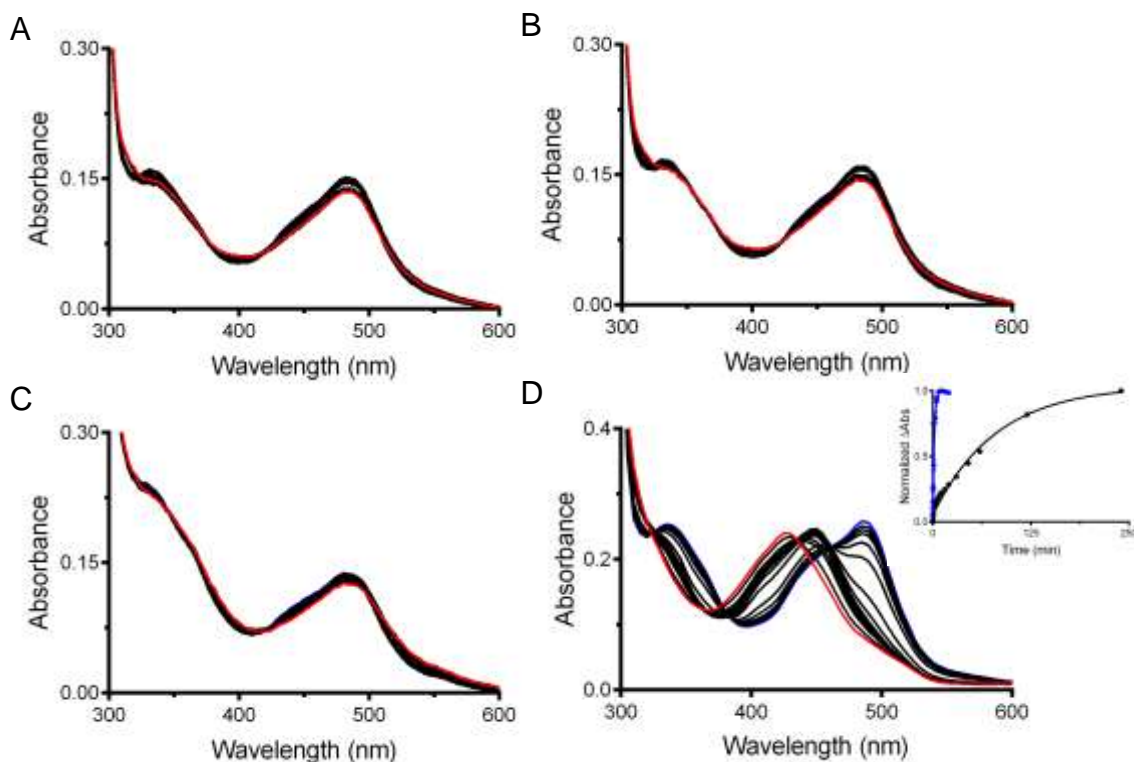


Figure S8. Photoejection of **4** (30 μM) followed by UV/Vis absorption spectroscopy in different media; (A) water, (B) 1X PBS, (C) Opti-MEM with 1% FBS, (D) CH_3CN . The blue line is the initial and the red line is the final spectra. Inset: The kinetics curve was produced by monitoring the change in absorbance at 450-485 nm (blue) and 430-450 nm (black) and fit with a one phase decay equation using GraphPad Prism software.

Table S3. Half-lives ($t_{1/2}$) for photoejection for **2**.

Condition	$t_{1/2}$ (min) ^a
Water	0.6 ± 0.1 and 58 ± 12
1X PBS	0.6 ± 0.1 and 32 ± 3
Opti-MEM with 1% FBS	0.6 ± 0.1
Acetonitrile	0.07 ± 0.02 and 2.5 ± 0.5

^aKinetics were determined using the change in absorbance at 470-440 nm for aqueous conditions and 425-445 nm for acetonitrile and fit to a two phase decay except for Opti-MEM, which was fit to a one phase decay equation.

Table S4. Δ_{abs} of photoejection for **3**.

Condition	Δ_{abs} @ 470 nm
Water	0.028 ± 0.001
1X PBS	0.038 ± 0.002
Opti-MEM with 1% FBS	0.041 ± 0.006
Acetonitrile ^a	0.15 ± 0.02 and 7.8 ± 0.5

^aKinetics were determined using the changes in absorbance at 475-440 nm for the initial fast phase and 425-440 nm for the slow phase and fit to a one phase decay.

Table S5. Δ_{abs} of photoejection for **4**.

Condition	Δ_{abs} @ 485 nm
Water	0.012 ± 0.001
1X PBS	0.013 ± 0.001
Opti-MEM with 1% FBS	0.012 ± 0.003
Acetonitrile ^a	1.3 ± 0.2 and 55.8 ± 0.3

^aKinetics were determined using the changes in absorbance at 450-485 nm for the initial fast phase and 430-450 nm for the slow phase and fit to a one phase decay.

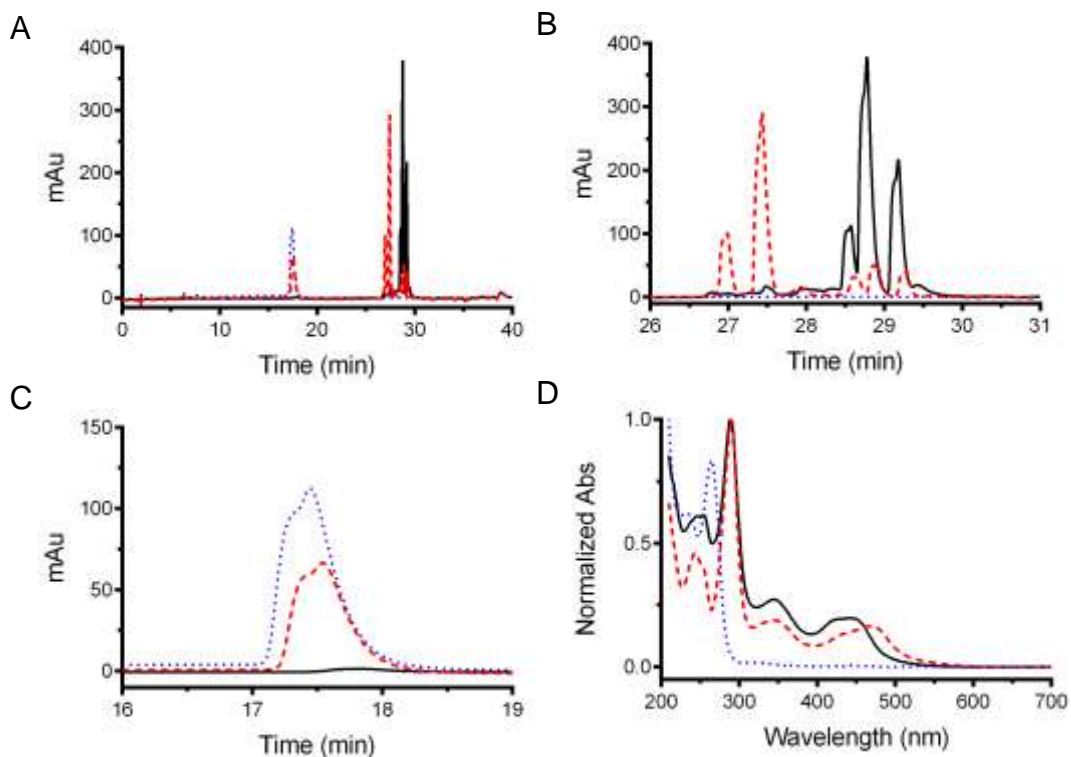


Figure S9. HPLC chromatograms of **2** in the dark and after 1 min irradiation with 470 nm light. For all graphs black (—): **2** in the dark, red (---): **2** after 1 min irradiation, blue (---): metyrapone. (A) Full HPLC chromatograms, where 17.5 min = free metyrapone, 26.5–27.8 min = **2** after 1 min irradiation, 28.5–29.5 min = **2**. Intact complex **2** has three peaks with the same absorption profiles due to the presence of the different isomers. (B) Ru(II) complex region of the HPLC chromatograms showing decreased signal for intact complex (26.5–27.8 min) and onset of shorter retention time products (28.5–29.5 min) following irradiation. (C) Metyrapone region of the HPLC chromatograms showing appearance of the signal in the irradiated sample. (D) UV/Vis absorption traces of the peaks showing a red-shifted MLCT band of **2** when irradiated with light. Extent of the photoejection reaction is 53%.

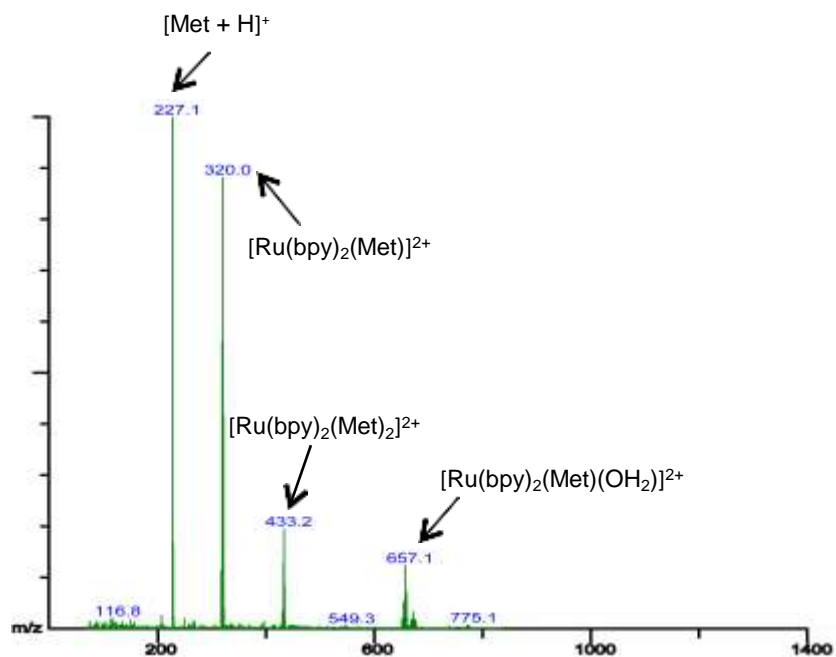


Figure S10. ESI-MS of **2** after being irradiated with 470 nm light. Ejection of one metyrapone ligand was confirmed by appearance of the peaks corresponding to free ligand and $[Ru(bpy)_2(Met)]^{2+}$ or $[Ru(bpy)_2(Met)(H_2O)]^{2+}$, as well as the reduction in the signal of the intact complex.

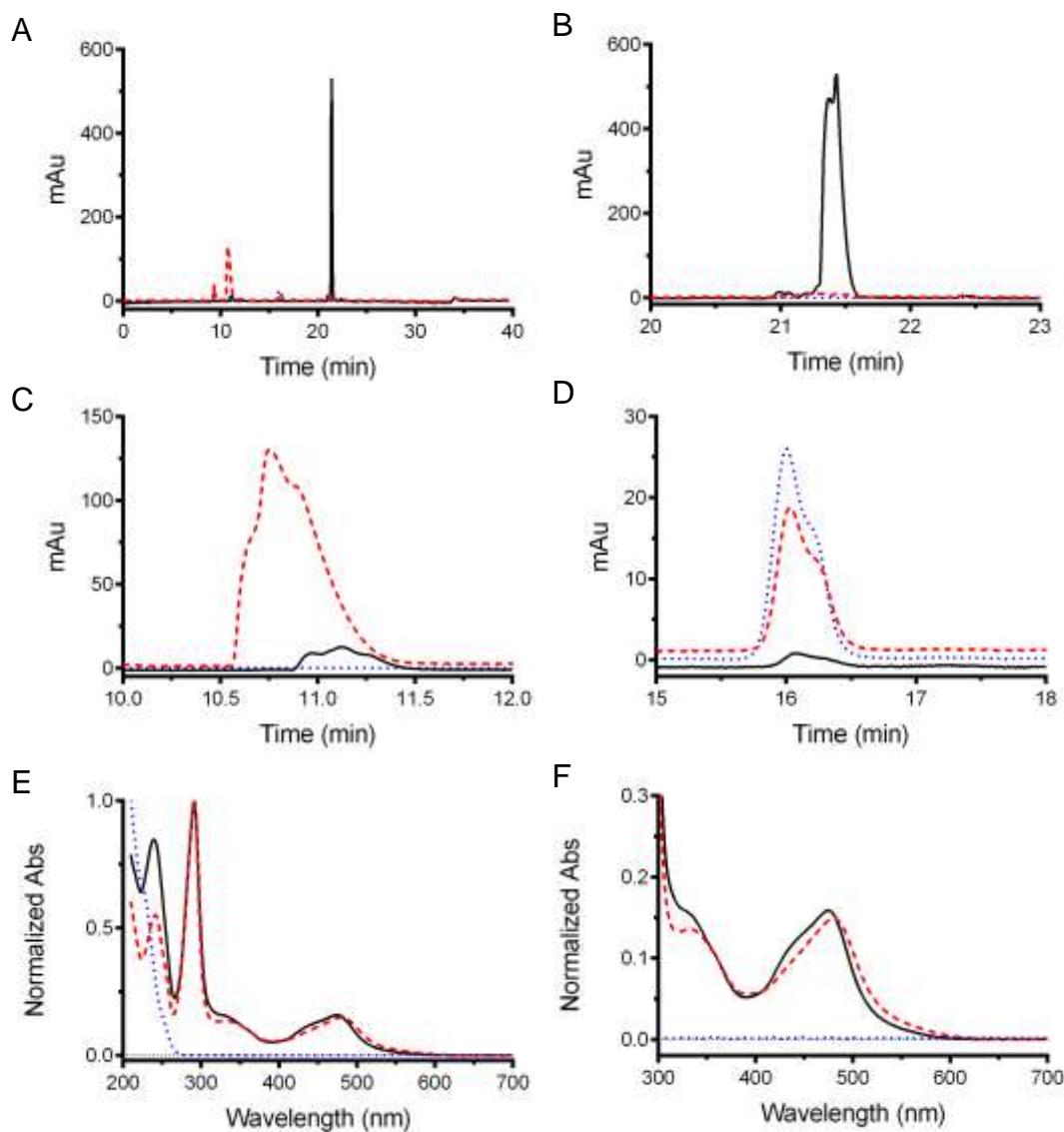


Figure S11. HPLC chromatograms of **3** in the dark and after 1 min irradiation with 470 nm light. For all figures black (—): **3** in the dark, red (---): **3** after 1 min irradiation, blue (---): etomidate. (A) Full HPLC chromatograms, where 11 min = **3** after 1 min irradiation, 16 min = free etomidate, 21.5 min = **3** in the dark). (B) Intact **3** region of the HPLC chromatograms showing decreased signal following irradiation. (C) Irradiated product region of the HPLC chromatograms showing increased signal following irradiation. (D) Etomidate region of the HPLC chromatograms showing appearance of free ligand following irradiation. (E) Full and (F) zoomed UV/Vis absorption traces of the peaks showing a slight red-shifted MLCT band of **3** when irradiated with light. Extent of the photoejection reaction is 65%.

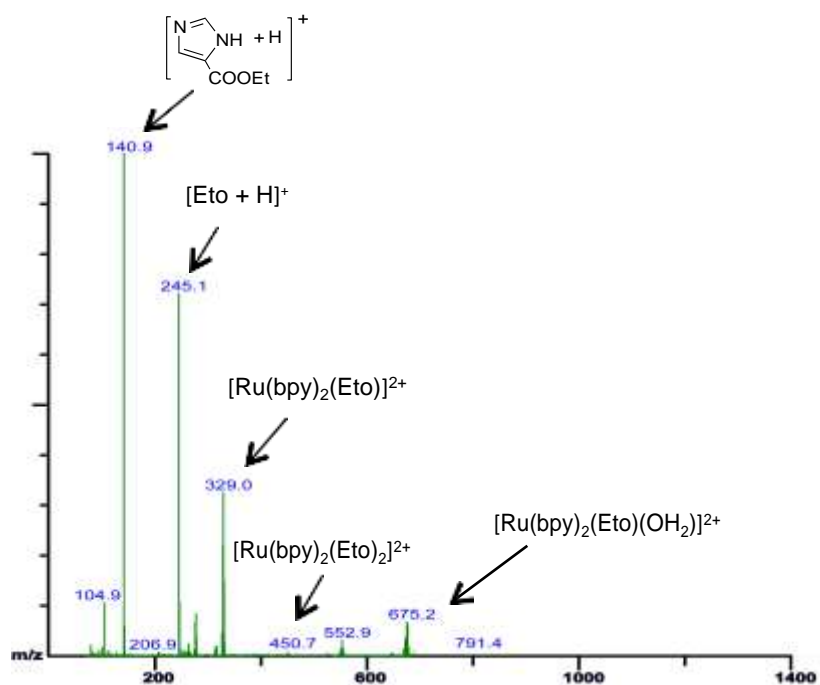


Figure S12. ESI-MS of **3** after being irradiated with 470 nm light. Ejection of one etomidate ligand was confirmed by appearance of the peaks corresponding to free ligand and [Ru(bpy)₂(Eto)]²⁺ or [Ru(bpy)₂(Eto)(H₂O)]²⁺, as well as the reduction in the signal of the intact complex.

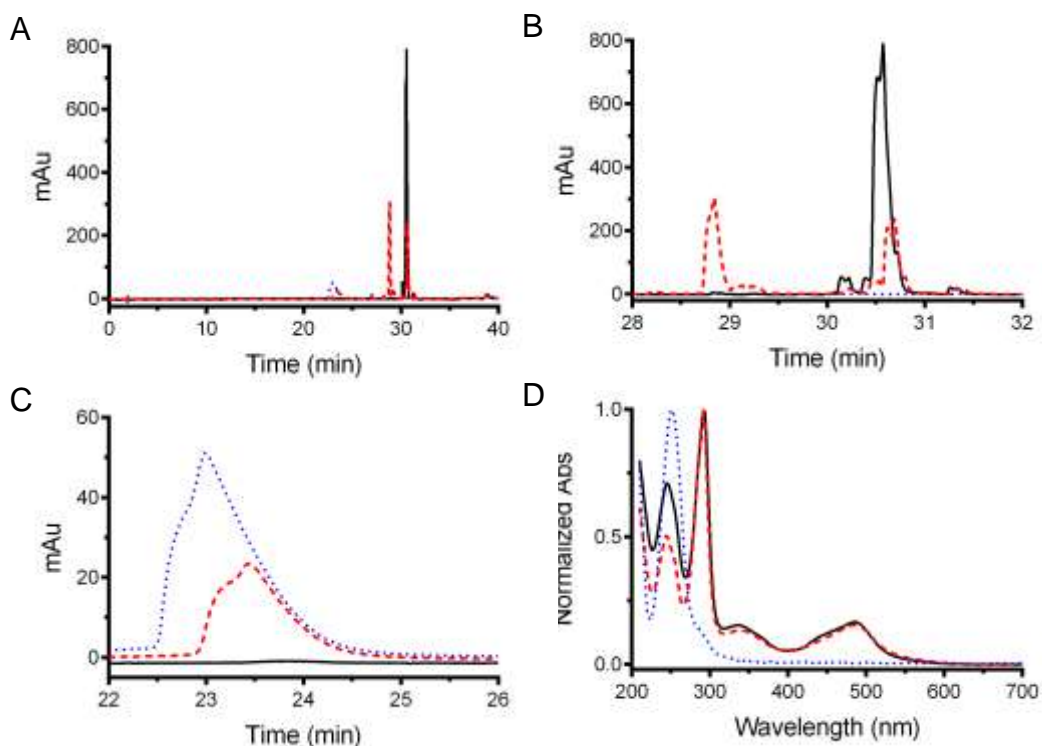


Figure S13. HPLC chromatograms of **4** in the dark and after 1 min irradiation with 470 nm light. For each figure black (—): **4** in the dark, red (---): **3** after 1 min irradiation, blue (---): **1**. (A) Full HPLC chromatograms, where 23 min = **1**, 28.8 min = **4** after 1 min irradiation, 30.6 min = **4** in the dark. (B) Ru(II) complex region of the HPLC chromatograms showing decreased signal for intact **4** and appearance of the Ru(II) product following irradiation. (C) Compound **1** region of the HPLC chromatograms showing the appearance of the signal following irradiation. (D) Full UV/Vis absorption traces of the peaks showing slight changes in the MLCT band of **4** when irradiated with light. Extent of the photoejection reaction is 40%.

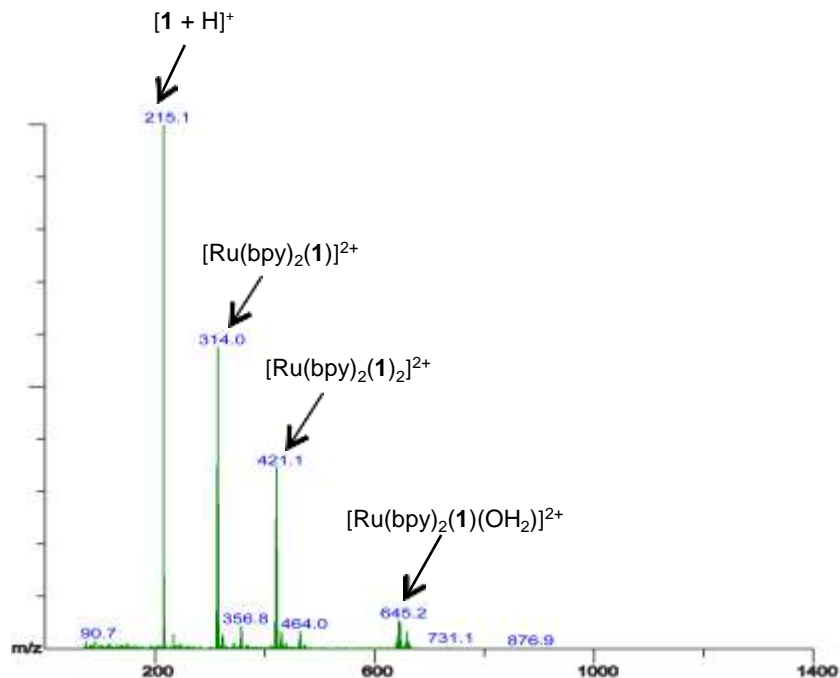


Figure S14. ESI-MS of **4** after being irradiated with 470 nm light. Ejection of one **1** ligand was confirmed by appearance of the peaks corresponding to free ligand and $[\text{Ru}(\text{bpy})_2(\mathbf{1})]^{2+}$ or $[\text{Ru}(\text{bpy})_2(\mathbf{1})(\text{H}_2\text{O})]^{2+}$, as well as the reduction in the signal of the intact complex.

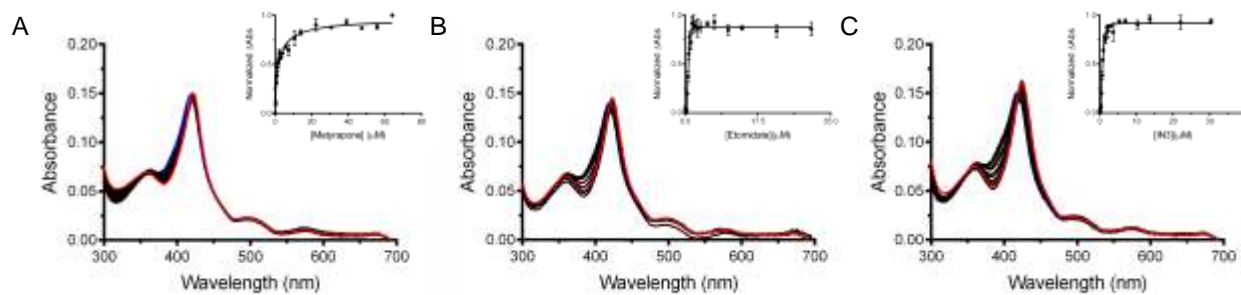


Figure S15. UV/Vis spectral traces of PM BM3 (2.5 μM) at RT in assay buffer with increasing ligand concentration: (A) metyrapone, (B) etomidate, (C) and **1**. The blue line is the initial and the red line is the final spectra. Inset: The binding curves were produced by monitoring the change in absorbance at 425 nm and fit with a one site-total non-linear equation using GraphPad Prism software.

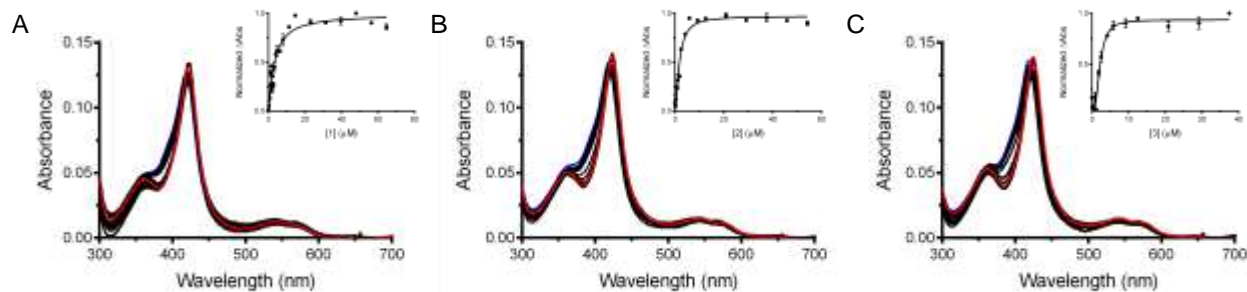


Figure S16. UV/Vis spectral traces of PM BM3 (2.5 μM) at RT in assay buffer with increasing concentration of complexes: (A) **2**, (B) **3**, and (C) **4** after irradiation with the Indigo LED. The blue line is the initial and the red line is the final spectra. Inset: The binding curves were produced by monitoring the change in absorbance at 425 nm and fit with a one site-total non-linear equation using GraphPad Prism software.

Table S6. K_d values for ligands and light-activated complexes.

Ligand	K_d (μM)	Complex	K_d (μM)
Metyrapone	1.09 ± 0.18	2	6.13 ± 1.46
Etomidate	0.83 ± 0.22	3	3.20 ± 0.59
1	0.93 ± 0.18	4	4.63 ± 1.75

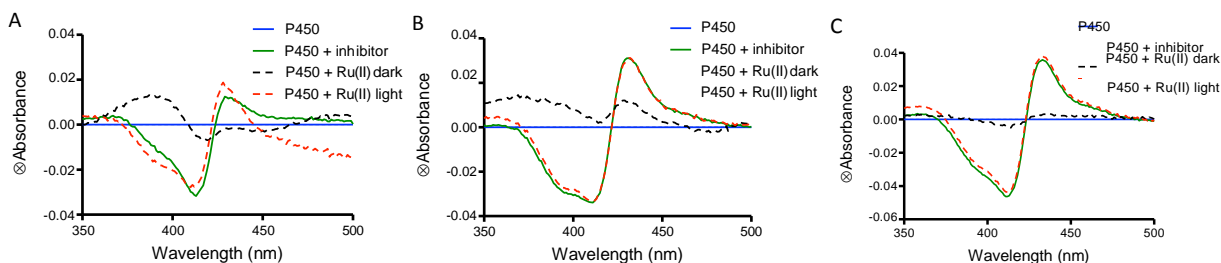


Figure S17. Difference spectra of P450_{BM3} inhibitor saturated and Ru(II) dark and light systems: **2** (A), **3** (B), **4** (C). The ratio used was P450: Complex (1:10) and P450: Ligand (1:4) for each of the respective ligands used to generate the complexes. The absolute spectra are shown in Figure 1.

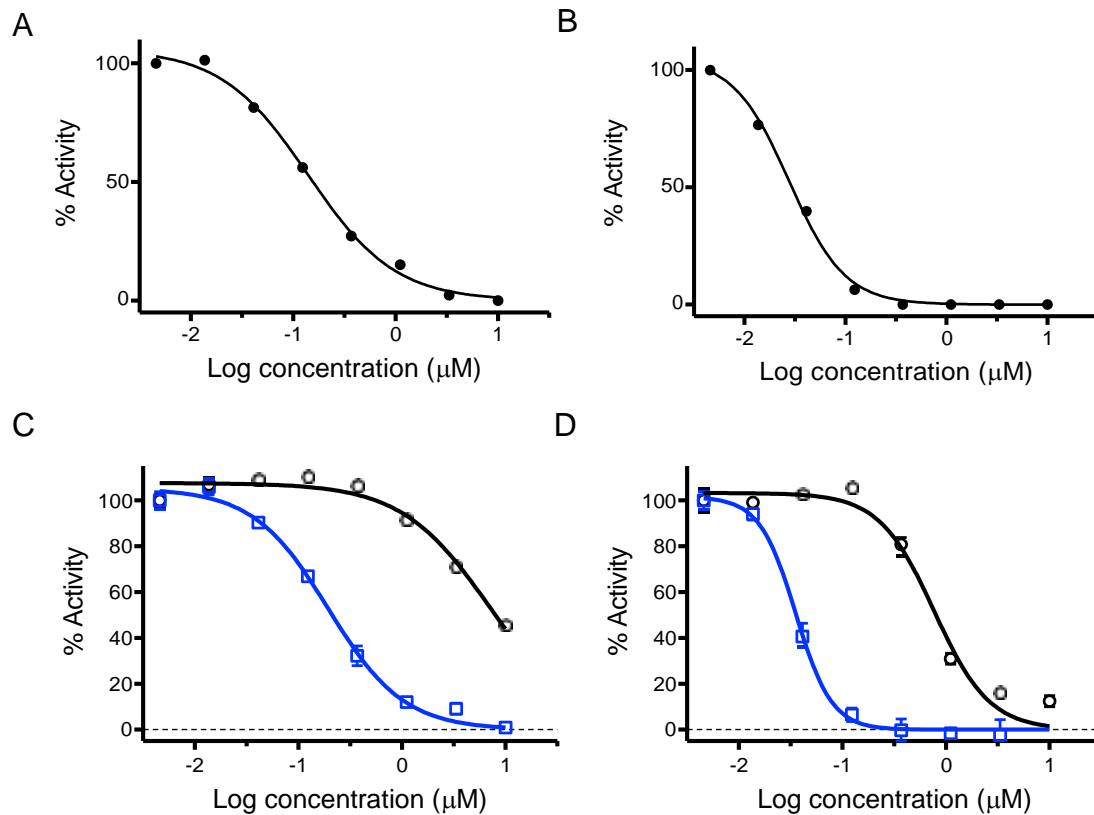


Figure S18. P450_{BM3} activity assay for (A) metyrapone, (B) etomidate, (C) **2** and (D) **3**, For (C) and (D), complexes **2** and **3** were tested in the absence of light (—) and following 1 min of irradiation with the Indigo LED (—).

Table S7. P450_{BM3} activity assay IC₅₀ values.

Ligand	IC ₅₀ (μM)	Complexes	IC ₅₀ (μM) ^a
Metyrapone	0.75 ± 0.43	2	0.19 ± 0.02 3.47 ± 0.74
Etodimate	0.02 ± 0.00	3	0.04 ± 0.01 0.61 ± 0.05
1	0.06 ± 0.03	4	0.05 ± 0.00 6.82 ± 2.06

^a Values listed first in black are light activated complexes. Values listed in blue, are IC₅₀ values for complexes in the dark.

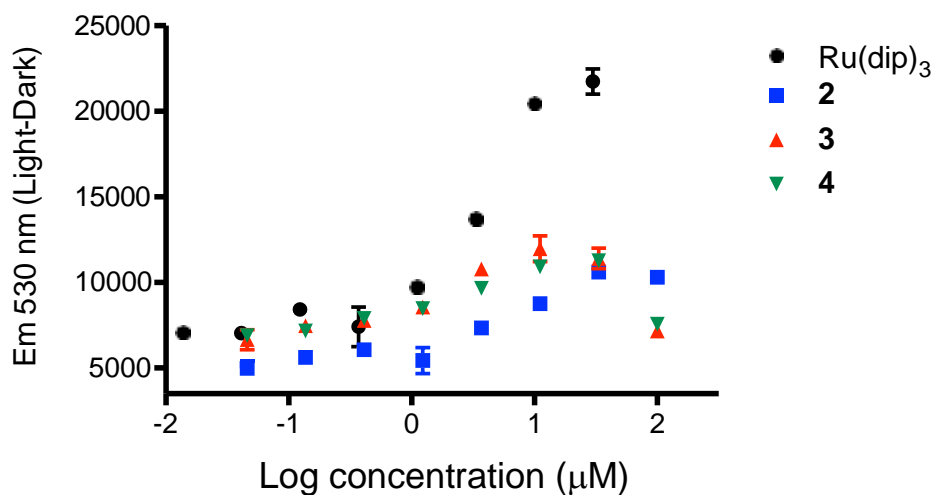


Figure S19. Singlet Oxygen Sensor Green detection of $^1\text{O}_2$ demonstrated low levels are produced by complexes **2–4**. $\text{Ru}(\text{dip})_3$ (dip=bathophenanthroline) was used as a control.

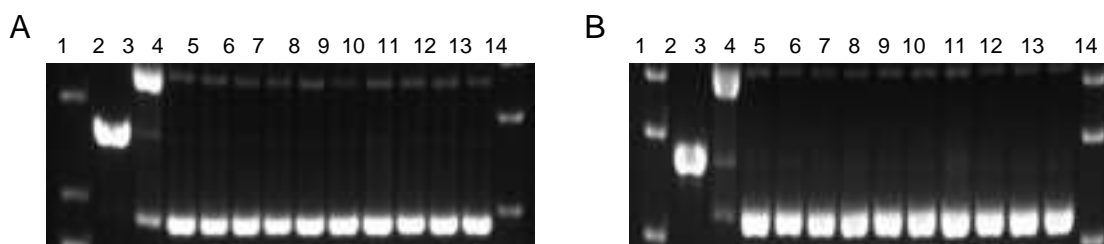


Figure S20. Agarose gels showing the dose response of ligands with 40 $\mu\text{g}/\text{mL}$ pUC19 plasmid with and without irradiation (470 nm). (A) Dark and (B) 3 hr irradiation. Lane 1 and 14: DNA ladder; Lane 2: EcoRI; Lane 3: $\text{Cu}(\text{OP})_2$; Lane 4: 0 mM, Lanes 5–7: 7.8, 62.5, 500 mM metyrapone; Lanes 8–10: 7.8, 62.5, 500 mM etomidate; Lanes 11–13: 7.8, 62.5, 500 mM **1**. EcoRI and $\text{Cu}(\text{OP})_2$ are used as controls for linear and relaxed circular DNA, respectively. EtBr was used to visualize the DNA.